

Improving Attachments of Non-Invasive (Type III) Electronic Data Loggers to Cetaceans

Michael Moore, Alex Shorter, Tom Hurst, and Alessandro Bocconcelli
Woods Hole Oceanographic Institution
Woods Hole, MA 02543
phone: 508 289 3228 fax 508 457 2089 email: mmoore@whoi.edu

Mark Johnson & Peter Tyack
Sea Mammal Research Unit, University of St. Andrews, Gatty Marine Laboratory, St Andrews, Fife
KY16 8LB UK

Dan Rittschof & Douglas Nowacek
Nicholas School of the Environment
135 Duke Marine Lab. Rd.
Beaufort, SC 28516

Laurens Howle
BelleQuant Engineering PLLC
7813 Dairy Ridge Rd.
Mebane, NC 27302

Award Number: N00014-11-1-0113
<http://www.whoi.edu>

LONG-TERM GOALS

The overall goal of this project is to increase the longevity of suction cup attachments for short term archival tags such as the DTAG. Specifically, we are working to extend the routine attachment duration for suction-cup tags to multiple days, if not weeks.

OBJECTIVES

- 1) Examine and identify forces and failure modes in suction cup attachments.
- 2) Assess the impact of tags and non-invasive surface attachments on cetaceans.
- 3) Take the knowledge gained from objectives 1) and 2) and engineer suction cups and surface treatments for improved attachment.
- 4) Examine on-animal performance of engineered attachments and tags.

APPROACH

Our approach is divided into four subtasks:

Task I: Forces and failure modes in suction cup attachments. Define assays to investigate cup failure modes.

Task II: Assessing the impact of tags and surface attachments on cetaceans. Using Computational Fluid Dynamics we will assess the drag forces created by various suction cup and tag housing combinations.

Task III: Engineered suction cups and surface treatments for improved attachment. In the light of Tasks I and II we will engineer suction cups with longer duration using selected materials and molding techniques, cup surface treatments, and investigate the use of adhesives.

Task IV: On-animal performance of engineered attachments and tags. Using free swimming animals, first in captivity and then on stranded releases and animals tagged at sea, we will attach the engineered system with an instrumented cup to test cup behavior and longevity.

WORK COMPLETED

TASK I: Evaluation of the Material Properties of Cetacean Skin with an Instrumented Cup

Objective: Design and experimental demonstration of a custom measurement tool, termed the smart static suction cup (SSSCup), to facilitate the investigation of vacuum loading on cetacean skin. The SSSCup enables the quantification of marine mammal skin compliance under vacuum loading for the first time.

Method: The SSSCup (Figure 1) consists of a rigid acrylic half-dome, a molded silicone lip, a linear variable differential transformer (LVDT) to measure displacement of the skin (LT0617, Active Sensors, USA), a pressure sensor (US300, Measurement Specialties, USA) and two thermistors (192-102DEW-A01, Honeywell, USA). A peristaltic pump (200 series, Williamson Manufacturing, UK) creates a controllable vacuum force in the cup and is attached via flexible tubing to a pressure port on the top of the SSSCup. Sensor data are logged using a netbook and USB analog to digital converter (U6, LabJack U6). Initial testing of the SSSCup was conducted on a common dolphin (*Delphinus delphis*) cadaver that had been frozen shortly after death, Further testing was conducted at the Chicago Zoological Society, Sarasota Dolphin Research Program's health assessment (May 2012).

The SSSCup was used to examine three sites with varying anatomical substructure on both the live animals and the cadaver: Site (1) a location with significant subcutaneous fat; Site (2) overlies muscle inserting on the blade of the scapula; and Site (3) has increased blubber fiber content as part of the dorsal fin saddle, Figure 2. Three vacuum loading profiles were used to characterize the response of the skin at each site, Figure 3. **Test 1**, a step vacuum loading was increased and then decreased to a 0.3 bar differential. **Test 2**, repetitive pressure loading was used to examine the response of the skin over three pressure ranges: low (0.5-0.1 bar), medium (0.5-2 bar), and high (0.5 to 3 bar). **Test 3**, static loading at a single pressure differential (0.3 bar) was used to characterize creep and relaxation of the skin. To explore individual component behavior of the anatomical substructure of the skin (skin, blubber, fat and muscle) under a vacuum force, a non-metallic version of the SSSCup was applied to the cadaver with a 0.1 bar pressure differential (comparable to a DTAG cup differential) during a

computed tomography (CT) scan of the cup/animal system. Scanning was conducted in the Computerized Scanning and Imaging (CSI) facility at the Woods Hole Oceanographic Institution.

IMPACT/APPLICATIONS

Acknowledgement: Many thanks to Randall Wells, and the Chicago Zoological Society's Sarasota Dolphin Research Program for the opportunity to undertake this work with free-ranging bottlenose dolphins, under Scientific Research Permit N0. 15543. Other work was conducted under NOAA permit 14241 issued to Dr Peter Tyack.

TASK II: CFD modeling for improved tag design

Objective: Tag packaging must be hydrodynamic to minimize the forces generated by fluid flow. As such, drag loading of suction cup tag designs was analyzed using a computational fluid dynamics (CFD) model. Two housing designs were analyzed using CFD simulations: 1) an existing tag housing design (Model A); 2), a biologically-inspired tag housing design (Model B), Figure 9. Simulated results for the Model A and B tags were experimentally verified in a water tunnel.

Method:

Simulations: A CFD model was used to analyze the forces acting on the designs over a range of flow velocities (0.25-10 m/s) and flow orientations (0-180 deg) during steady RANS flow field simulations using the SolidWorks 2011 Flow Simulation package.

Experimental Validation: Water tunnel experiments were conducted at the United States Naval Academy in Annapolis, Maryland. Full-scale models of the two tag designs were made from ABS plastic using fused deposition modeling (FDM), Figure 10. Models were evaluated in flow speeds ranging from 1 m/s to 5.5 m/s, and orientations ranging from -20 to +90 degrees (with the zero angle indicating tag alignment with the flow). Measurements of lift, drag, and side force were made with submersible Hydronautics force transducers and the angle of the model was measured by a multi-turn potentiometer mounted on a custom built quadrant.

TASK III: Engineered suction cups and surface treatments for improved attachment: The use of adhesives to improve cup performance

Objective: Utilize a rapid curing topical glue to extend the reliable longevity of noninvasive tag attachments to multiple days without harmful effects to the animal. Test results from shear and tensile adhesive failure of pseudobarnacles (Figure 12) attached to dolphin skin (*Tursiops truncatus*) with cyanoacrylate (Loctite liquid professional Super Glue) are presented here.

Method: An ASTM standard method (Anonymous, 1997) was used to determine removal force in shear of pseudobarnacles. The pseudobarnacles consisted of stainless steel bolts (3/8 x 2½) and vinyl from a Hedstrom (54-3303W) play ball. The head of the pseudobarnacle had a radius of 6.5 mm corresponding to a 130 mm² area of attachment with the substrate. A small nut (3/8-16) was screwed onto the bolt until flush with the edge of the bolt to provide a suitable feature for normal loading of the pseudobarnacle. Frozen dolphin skin (*Tursiops truncatus*) that had been thawed overnight was used for the attachment surface. The skin was cleaned with a damp towel before the application of the pseudobarnacles.

One drop (30ul) of liquid super glue was applied to the vinyl section of the pseudobarnacle, and then placed onto the skin without additional force. After 30 seconds curing under its own weight, the removal force was tested. The shear force required to remove the pseudobarnacle was created by pushing in a horizontal direction as close to the skin as possible with a 20 lbs capacity Shimpo MF-20 force gauge. Normal force loading was created using a Vernier dual range force sensor (Logger Pro 3.8.4.2) with the hook attachment. Twenty trials were conducted in both loading directions, each in new locations on the skin.

Acknowledgement: Many thanks to Pablo Valdivia and Michael C. Farruggia.

PLANNED YEAR 3 WORK

In year three, we will continue to advance the objectives of the project: (1) identification of critical factors that lead to type III attachment failure; (2) improved type III designs that maximize attachment reliability and minimize disturbance to the host animal; (3) quantification of the energetic implications of a type III tag on small cetaceans. Continued testing with the SSSCup and measurements of suction cup performance during attachment on free-swimming animals will facilitate the identification of failure modes for type III attachments. The CFD modeling work from Task II will directly inform new hydrodynamic tag housing designs, and prototype tags that utilize glue for improved attachment durations will be developed. Finally, we will be undertaking experimental work with captive dolphins to quantify energetic cost associated with type III tags. Simultaneously, the results from the project will be shared through presentations at scientific conferences and in peer reviewed journal publications. Currently, the SSSCup work will be presented at the American Society of Biomechanics 2012 meeting in Gainesville Florida, and a manuscript describing the CFD modeling work is in preparation (details are provided below).

RESULTS

TASK I: The CT images of the SSSCup on the common dolphin cadaver (Figure 4) provide snap shots of the response of the animal skin during vacuum loading. The 0.1 bar loading creates a visible deformation compared to the unloaded side of the animal. Measurements taken from the images show a change in thickness of the subcutaneous fat and a small change to the blubber thickness, but not to the skin itself, Table 1.

SSSCup Test 1: Figure 5 presents Force vs Displacement curves generated from the static step data at the three sites from the cadaver (left) and from 6 live bottlenose dolphins (right). For the cadaver, Site 3 (lateral fin) was the least compliant of the three, and the compliance of Sites 1 and 2 were comparable. All sites on the cadaver demonstrated hysteresis during unloading. For the live animals, the compliance trends observed in the cadaver data are also present, but there was less hysteresis and larger deflections in the live animal data at the three sites.

SSSCup Test 2: Figure 6 presents average data from the 5 repetitive loading cycles at the high pressure range conducted on the cadaver. Again, Site 3 (lateral fin) was the least compliant, while Sites 1 and 2 had comparable compliance (particularly at peak loading). The area in the center of each curve (or hysteresis loop) represents energy dissipated due to material visco-elasticity of the skin. Figure 7 compares the average energy absorbed by the skin during all the repetitive loading trials. During the medium and high trials, Site 3 absorbed the least energy, and the energy absorbed by Sites 1 and 2 were comparable. This trend did not hold for the low loading trials.

SSSCup Test 3: The skin at the three sites was loaded to 0.3 bar, allowed to reach a steady-state displacement, and then unloaded. The pump took ~40 s to reach 0.3 bar during the initial loading, but the pressure release took ~1sec (Figure 8). Again, Sites 1 and 2 had larger overall displacements than Site 3. However, both the creep and relaxation times to 95% of steady-state were comparable for the three sites, Table 2.

TASK II: Experimental results confirmed the trends observed in the simulation studies, Figure 11. The measured drag matched the simulated drag closely at all orientations with an RMS difference of 1 N, averaging over all 5 test speeds and orientations. The difference between the simulated and experimental lift forces was substantially larger with RMS differences of 13.8 N and 10.7 N for Model A and B. Lift was the dominant force component acting on both tag designs in the water tunnel. At the fastest experimental speed (5.6 m/s), the lift was 61 N and 74 N on Model A and B, respectively. The measured drag force was closer to the simulated values with 14 N and 4 N measured for Model A and B, respectively, at 5.6 m/s, resulting in calculated drag coefficients of 0.4 and 0.09 for the two shapes. The variation in force with flow speed followed closely the speed-squared law predicted by simulations for both tag designs.

TASK III: The average shear force that resulted in adhesive failure was 7.3 N (0.055MPa), with a minimum and maximum force of 4 N (0.030 Mpa) and 12.5 N (0.094 MPa), respectively (Figure 13). An average normal force of 4.5 N (0.034 Mpa) was required to remove the anchor from dolphin skin. The minimum and maximum normal force observed were 2.1 N (0.016 MPa) and 7.5 N (0.057 MPa), respectively (Figure 13). Vinyl was used as the interface material between the bolt and the skin in order to enable engineering of cohesive rather than adhesive failure to insure that the material failed instead of damaging the skin. Silicone has also been shown to be suitable interface material.

SUMMARY: The SSSCup described in **Task I** enables the quantification of marine mammal skin compliance under vacuum loading for the first time. SSSCup measurements demonstrated that there are notable differences in compliance, hysteresis, and energy absorption of the skin between the three test sites on the cadaver. In particular, the static cup studies showed less compliance, displacement, and energy absorption lateral to the dorsal fin (Site 3), than further anterior (Sites 1 and 2). However, the creep and relaxation response times were similar between the sites. The CT studies demonstrate that an important determinant of epidermal deformation by a suction cup is the amount of underlying subcutaneous fat.

The modeling work presented in **Task II** provides insight into hydrodynamic housing design and the resulting drag forces for large whale bio-logging tags. In summary, these results demonstrated that a smooth form (Model B) reduced drag, and a small cross sectional area close to the attachment surface (Model A) reduced lift force acting on the tag body. Further, the results demonstrate experimentally that the lift component of the force was much greater than drag in both designs. Importantly, simulation results were validated experimentally with the overall trends measured during the experimental trials agreeing well with the simulations.

The preliminary results from the glue work presented in **Task III** demonstrate the potential for glue as a complimentary method of tag attachment. A suitable glue protocol using pseudobarnacles (Figure 12) was developed and used to quantify shear and tensile adhesive failure on dolphin cadaver skin. These preliminary results indicated that the cyanoacrylate tested provides an attachment force strong enough to secure a tag to an animal under the loading predicted by the **Task II** modeling work.

IMPACT/APPLICATIONS

TASK I: These results will be used to refine the assays to investigate cup failure modes. Data from the field results collected in conjunction with the Sarasota Dolphin Research Program are currently being analyzed and will also be used to inform future work with captive and stranded cetaceans when assessing the impact of the suction cup attachment on the animal. Additionally, the differences in material properties between live and dead animals will be examined to inform work that relies on data collected from cadavers.

TASK II: The computational modeling of the flow around the housing designs enabled the direct comparison of the forces acting on the tags. Importantly, experimental water tunnel testing was used to validate the simulation results, a requirement for CFD to be used to predict performance. A manuscript on the CFD modeling and experimental measurements is in preparation.

TASK III: The CFD simulations conducted for Task II of this project have predicted drag and lift forces on a tag as high as 50 N and 160 N in 10 m/s flow, respectively. For the tag modeled in the CFD simulations the attached area of a single compressed suction cups was $\sim 1963 \text{ mm}^2$ ($r = 25 \text{ mm}$), and the current design uses four cups giving a total area of attachment of 7850 mm^2 . Based on the experimental work presented above, a glue-only attachment over an area equivalent to the suction cup attachment area would secure the tag against drag forces up to 430 N and lift forces up to 267 N, greatly exceeding the forces predicted by the simulations. Further, we have identified and are now testing a silicone we can modify to enable cohesive failure. The use of silicone in place of vinyl will facilitate the integration of glue into current silicone suction cup designs.

REFERENCES

Anonymous, 1997. ASTM D 5618-94. Annual Book of ASTM Standards, vol. 06.02. ASTM, West Conshohocken, PA.

PUBLICATIONS

I. The following abstract has been accepted for the American Society of Biomechanics Annual meeting in Gainesville, Florida August 2012 - Suction and skin: the effect of vacuum loading on the skin of a common dolphin

Authors: ¹K. Alex Shorter, ²Tom Hurst, ³Mark Johnson, ²Scott Cramer, ²Darlene Ketten and ²Michael Moore

¹University of Michigan, Ann Arbor, MI, USA

²Woods Hole Oceanographic Institution, Woods Hole, MA, USA

³University of St. Andrews, St Andrews, Fife KY16 8LB, UK

Many marine mammals spend most of their life below the water surface, necessitating specialised observational tools to track their behaviour. To address this need, archival tags have been developed to collect and store high-resolution sound, image and motion data for intervals of hours or days [1]. Given the short recording duration of these devices, non-invasive attachment methods, such as suction cups, are frequently used to minimize animal impact [2].

Suction cups generate attachment force by balancing two forces acting perpendicular to the substrate: the shape restoring force of the distorted cup and the vacuum force created by the pressure difference between the ambient environment and the cup interior. During attachment, the lip is flattened and a majority of the air within the cup is expelled. When the attachment force is relaxed, the cup attempts to return to its original shape with the lip acting as a check valve preventing ingress of the surrounding fluid. Because the lip is sealed, the increase in internal volume resulting from the cup relaxation creates a reduced internal pressure and corresponding increase in vacuum force. The internal volume of the cup continues to expand until a balance is reached between the pressure force and the restoring force of the cup. As such, the vacuum force is dependent on the material/shape stiffness of the cup (i.e., the force with which it opposes shape distortion) and the properties of the substrate material (e.g. the animal's skin).

If the skin surface is less stiff than the cup, the skin may deform more than the cup in balancing the vacuum force. The performance of the attachment is then critically dependent on the surface and stress-strain properties of the skin and its ability to maintain stiffness against a static force. This work presents the design and experimental demonstration of a custom measurement tool, termed the smart static suction cup (SSSCup), to facilitate the investigation of vacuum loading on cetacean skin.

The instrumented SSSCup recorded a mean skin displacement of 1.0 cm into the SSSCup in the static and dynamic loading trials, Table 1. This confirms that the substrate plays an important role in suction generation and implies that the substrate properties will influence vacuum formation and maintenance. Figure 2 illustrates the nonlinear response of the skin to the applied pressure during one cycle of dynamic loading. A nonlinear stiffness was observed as the skin deformed rapidly at the onset of the loading (0 to 3 sec) and then at a reduced rate until the maximum pressure was reached at ~19 sec. Following the release of the pressure, the skin rapidly returned to its original state. Creep was not observed during the constant loading portions of the dynamic trials, as illustrated by Figure 2 or during the 1 hr extended loading test.

The CT images provide a snap shot of the response of the animal skin during vacuum loading, Figure 3. The -0.1 bar loading creates a visible deformation compared to the unloaded side of the animal. Measurements taken from the images show a change in thickness of the subcutaneous fat and a small change to the blubber thickness, but not to the skin itself, Table 2.

The measured displacement from the CT scan is comparable to the SSSCup measurement. The 0.3 cm difference observed in the measurements could be due to deformation created by the spring backed LVDT plunger tip and will be investigated in the future.

Direct measurement of the material properties of intact marine mammal skin will lead to improved performance of suction cups on marine mammals.

REFERENCES

1. Johnson M, Aguilar de Soto N, Madsen PT, (2009) Studying the behaviour and sensory ecology of marine mammals using acoustic recording tags. *Marine Ecology Progress Series*, 395:55-73.
2. Hooker SK, Baird RW (2001) Diving and ranging behaviour of odontocetes: a methodological review and critique. *Mamm Rev* 31:81-105.

II. The following manuscript is in preparation for submission to Marine Mammal Science.
Drag of suction cup tags on swimming animals: modeling and measurement

Authors: K. Alex Shorter¹, Laurens Howle², Mark Johnson³, Mark M. Murray⁴ and Michael Moore¹.

¹ Biology Department, Woods Hole Oceanographic Institution, Woods Hole, MA 02543, USA.

² Pratt School of Engineering, Duke University, Durham, NC 27708, USA and BelleQuant Engineering, PLLC, Mebane, NC 27302, USA.

³ Sea Mammal Research Unit, University of St. Andrews, Gatty Marine Laboratory, St Andrews, Fife KY16 8LB UK.

⁴ Mechanical Engineering Department, United States Naval Academy, 590 Holloway Road Annapolis, MD 21402, USA.

Key Words: Non-invasive, Tag Design, CFD, Bio-logging, Hydrodynamic

Abstract

The use of bio-logging tags for the study of marine mammals is becoming increasingly commonplace, and the development of hydrodynamic tag housings is a critical element of the design. Hydrodynamic housings reduce forces that can remove the tag or adversely affect the behavior or energetics of the animal. In this work, hydrodynamic loading of a current suction cup tag design (Model A), a modified design (Model B), and an idealized design (Model C) were analyzed using computational fluid dynamics (CFD) models. Importantly, the simulation results presented here were validated experimentally. Overall, the simulation and experimental results demonstrated that a tag housing that minimized geometric disruptions to the flow reduced drag forces, and that a tag housing with a small frontal cross-sectional area close to the attachment surface reduced lift forces. For all housing designs, off-axis flow increased the magnitude of the total force acting on the tag. Additionally, preliminary results from experimental work with a common dolphin cadaver indicate that the suction cups currently used to attach the types of tags described here provide sufficient attachment force to resist failure to predicted drag and lift forces in 10 m/s flow.

Table 1: Displacement measurements from CT scan.

Condition	Pressure (bar)	Displacement (cm)	Fat (cm)	Blubber (cm)	Skin (cm)
CT Cup	-0.1	1.3	1.3	1.1	0.1
CT Control	0	NA	1.0	1.2	0.1

Table 2: Time to 95% of steady-state for both loading and unloading during the Test 3.

	Site 1 (s)	Site 2 (s)	Site 3 (s)
Creep to 95% of Steady State	38	42	41
Relaxation to 95% of Steady State	2.9	2.9	2.7

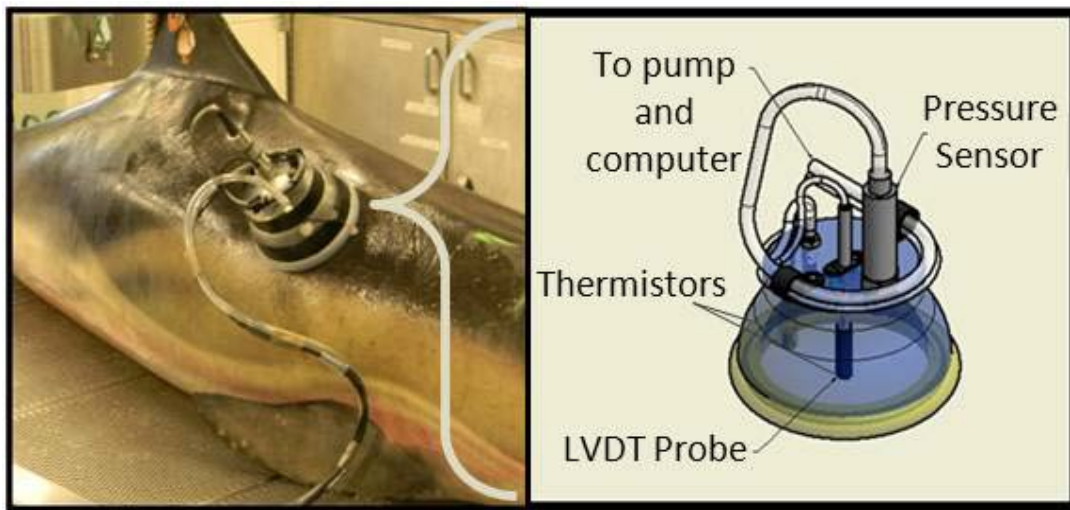


Figure 1: A mechanical drawing of the SSSCup assembly (right) and the SSSCup shown attached to the freshly stranded common dolphin cadaver (left).

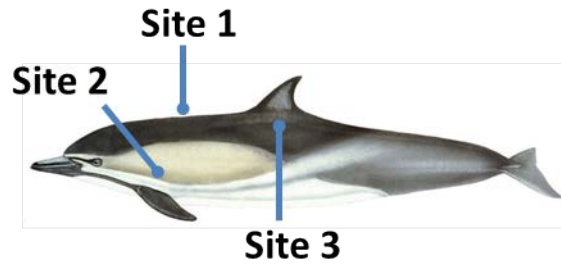
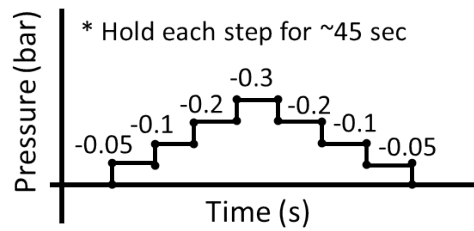
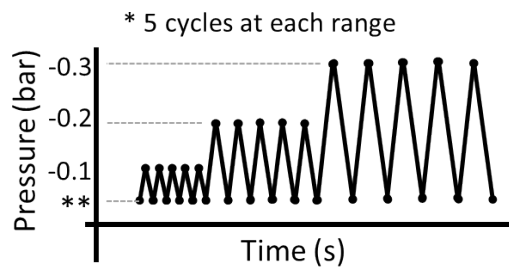


Figure 2: Test sites examined with the SSSCup: Site 1, dorsal midline; Site 2, lateral near the flipper insertion; and Site 3, lateral at the dorsal fin insertion.

Test 1: Static step pressure loading



Test 2: Repetitive Loading



Test 3: Creep and Relaxation

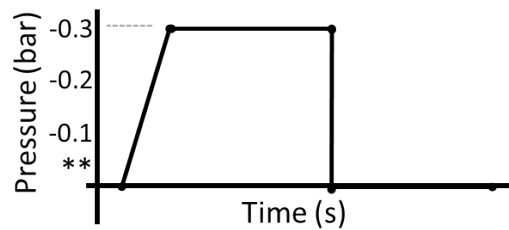


Figure 3: Pressure profiles used to characterize the dolphin skin using the SSSCup.

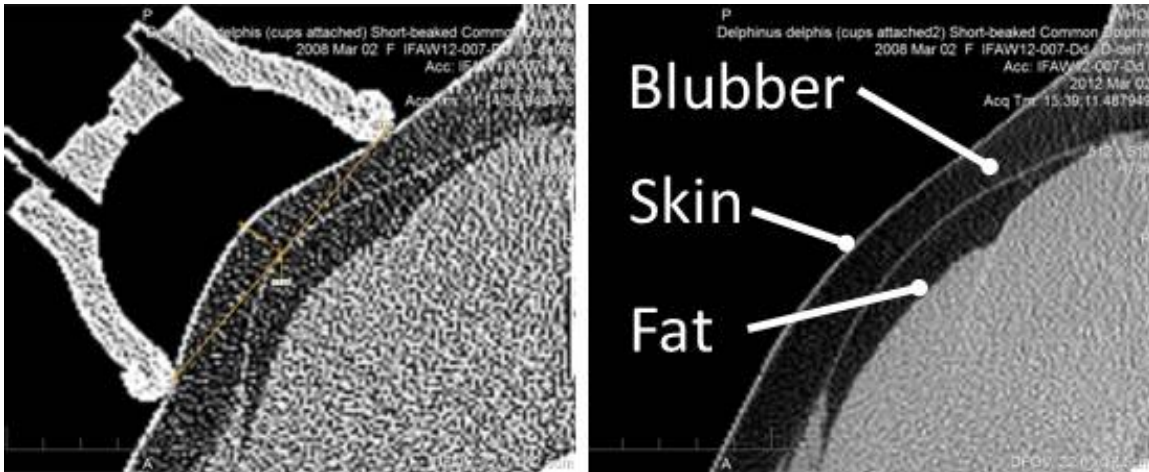


Figure 4: CT image of the non-metallic SSSCup (left) at -0.1 bar and the unloaded cadaver at the same site (right).

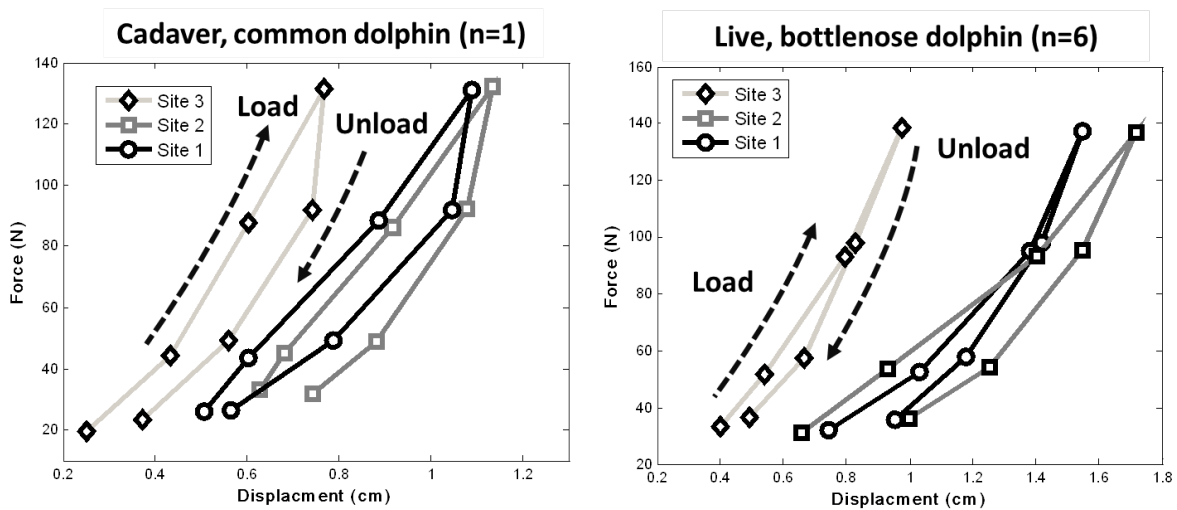


Figure 5: Steady-state displacements at the Dorsal Midline (Site 1), Lateral Flipper (Site 2), and Lateral Fin (Site 3). The figure shows the group average. The Lateral Fin was less compliant than the other two sites.

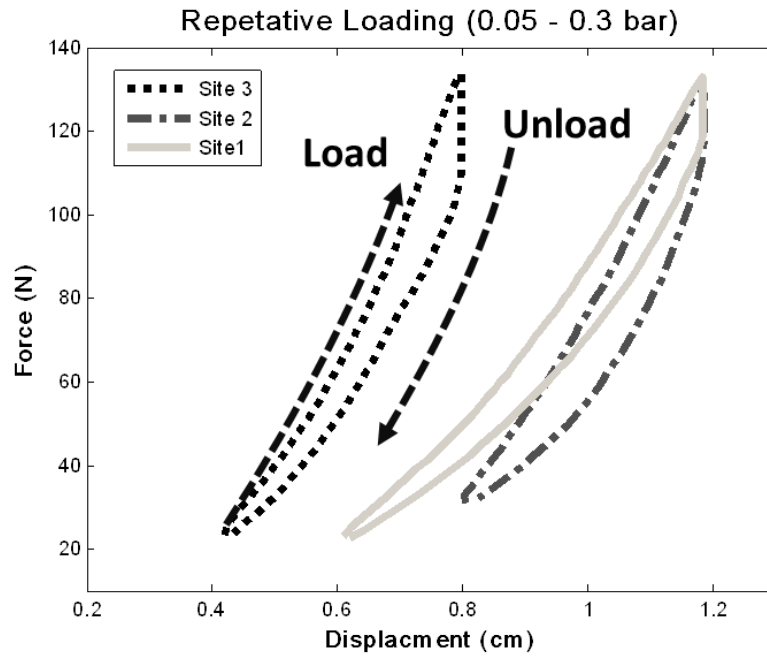


Figure 6: Displacement of the cadaver skin during repetitive loading at the three test sites during the highest level of repetitive loading (0.5-0.3 bar).

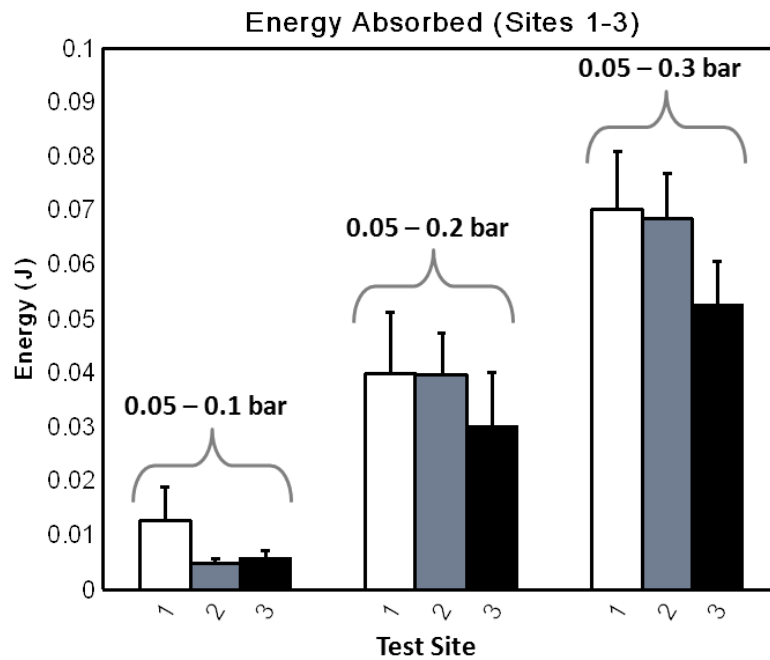


Figure 7: Energy absorbed by the skin during repetitive loading at the low (0.05-0.1 bar), medium (0.05-0.2 bar) and high (0.05-0.3 bar) loading ranges.

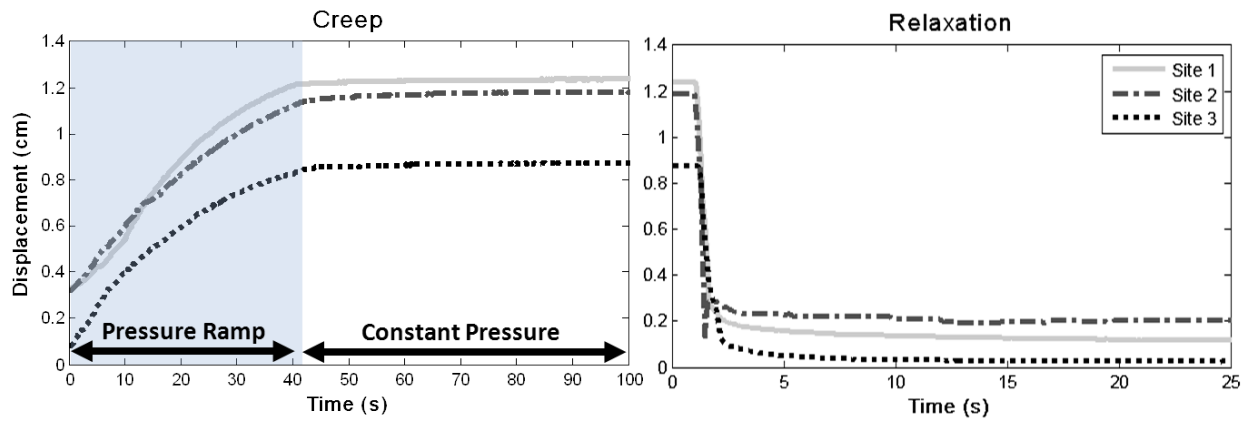


Figure 8: Right panel, displacement of the skin during the initial ramp loading and the subsequent 0.3 bar static pressure. The period of active pumping is indicated by the blue shading. Left panel, the relaxation of the skin after the 0.3 bar static pressure was released.

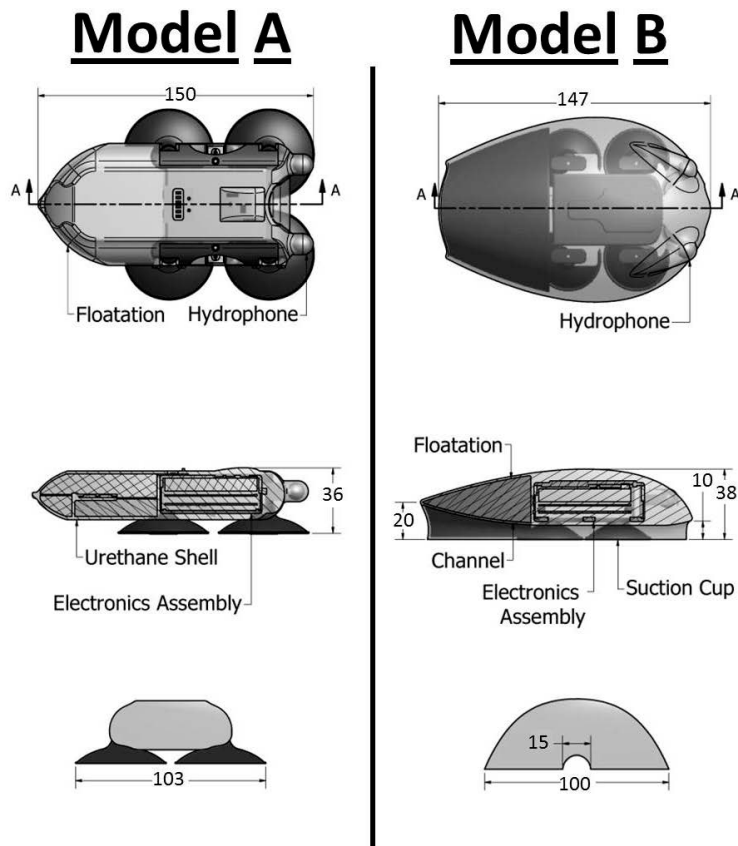


Figure 9 First column: Model-A tag geometry along with the largest cross section of the housing when the package is aligned with the direction of the flow (lower-left). Second column: Model-B tag geometry along with the largest cross section of the housing when the package is aligned with the flow (lower-right). A streamlined half-body provides a skirt around the cups to minimize geometric disruptions to the flow. All dimensions are in millimeters.

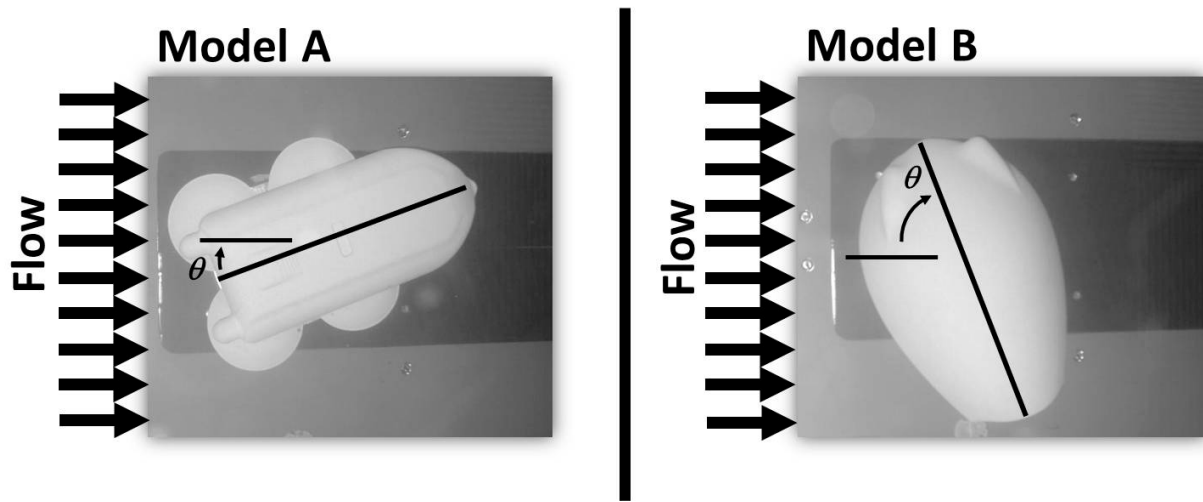


Figure 10 The solid models as seen from below in the water tunnel in two different orientations with respect to the flow. Fluid flow was from left to right as illustrated by the arrows.

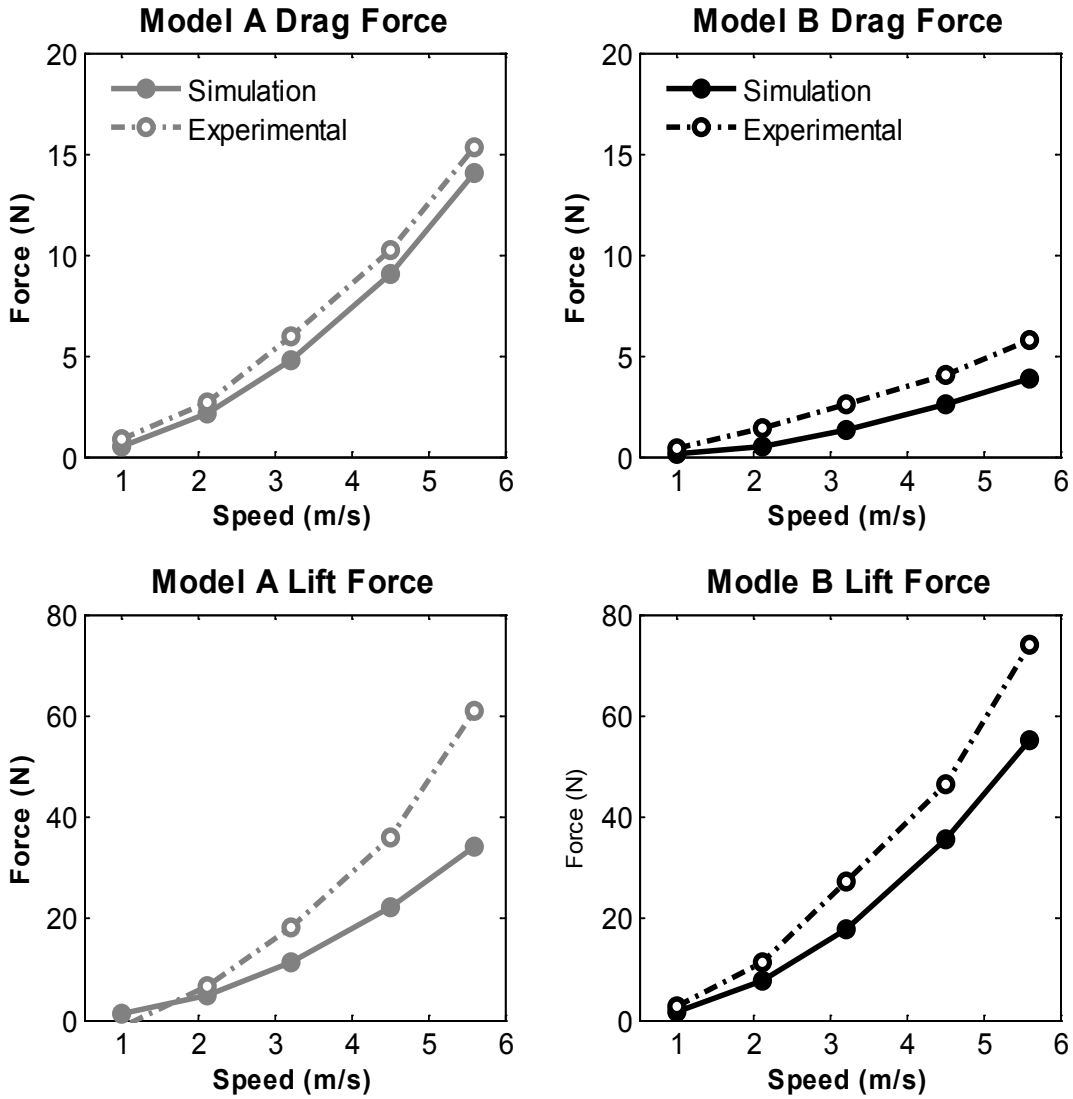


Figure 11 Experimental (solid with open circles) and simulated (dot-dashed with closed circles) results showing the drag and lift forces acting on the Model A (grey) and Model B (black) tag designs.

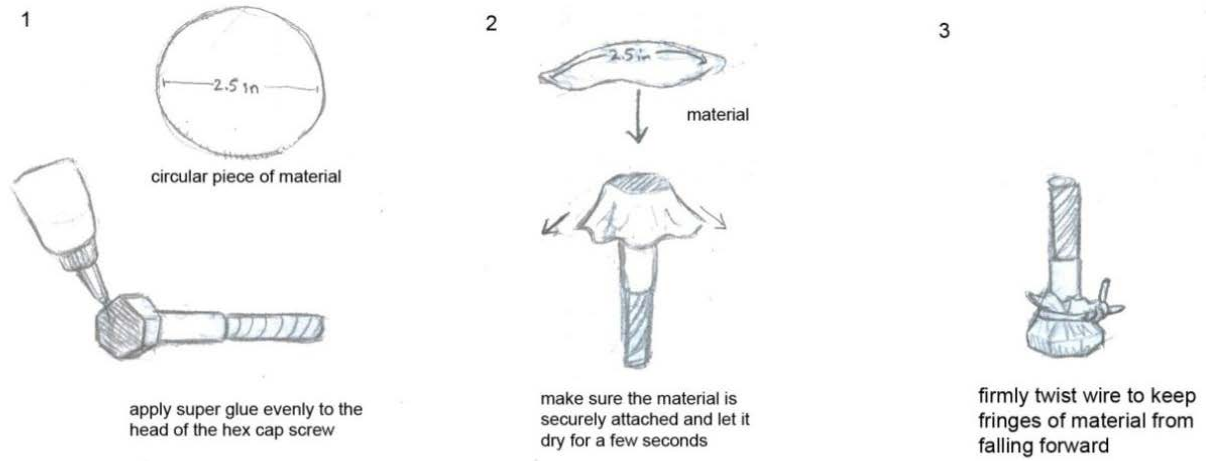


Figure 12 An illustration of the construction of a pseudobarnacle.

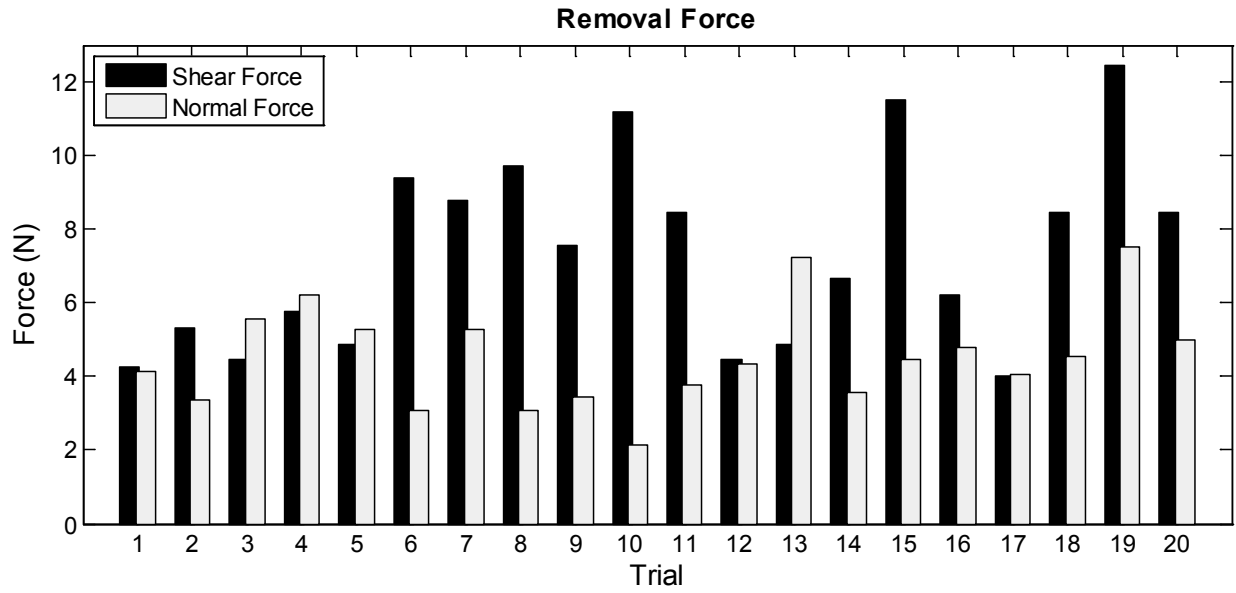


Figure 13 Experimental force results from the normal and shear testing of the pseudobarnacles.